Nuclear Inst. and Methods in Physics Research, A 899 (2018) 10–15

Contents lists available at ScienceDirect

Nuclear Inst. and Methods in Physics Research, A

journal homepage: www.elsevier.com/locate/nima

Ultimate position resolution of pixel clusters with binary readout for particle tracking

Fuyue Wang [a,b,*], Benjamin Nachman [b], Maurice Garcia-Sciveres [b]

[a] Department of Engineering Physics, Tsinghua University, Key Laboratory of Particle and Radiation Imaging, Ministry of Education, Beijing 100084, China
[b] Physics Division, Lawrence Berkeley National Laboratory, Berkeley, CA 94720, USA

ARTICLE INFO

Keywords:
Silicon pixel detector
Binary readout
Position resolution

ABSTRACT

Silicon tracking detectors can record the charge in each channel (analog or digital) or have only binary readout (hit or no hit). While there is significant literature on the position resolution obtained from interpolation of charge measurements, a comprehensive study of the resolution obtainable with binary readout is lacking. It is commonly assumed that the binary resolution is pitch/$\sqrt{12}$, but this is generally a worst case upper limit. In this paper we study, using simulation, the best achievable resolution for minimum ionizing particles in binary readout pixels. A wide range of incident angles and pixel sizes are simulated with a standalone code, using the Bichsel model for charge deposition. The results show how the resolution depends on angles and sensor geometry. Until the pixel pitch becomes so small as to be comparable to the distance between energy deposits in silicon, the resolution is always better, and in some cases much better, than pitch/$\sqrt{12}$.

1. Introduction

The spatial resolution of silicon strip and pixel detectors has been analyzed in detail before (see for example [1–3]). This prior work has focused on the resolution that can be obtained by interpolation of charge measurements in adjacent channels, on the charge deposition and transport processes, on signal to noise of the charge measurement, and on functional forms to calculate position from measured charges. However, the resolution limits in the case of binary readout (no charge information, just hit or no hit above a preset threshold) have not been fully explored. For example, it is commonly stated that a single channel hit has a spatial resolution of pitch/$\sqrt{12}$ — the standard deviation of a uniform random variable on the interval $[0, \text{pitch}]$, but this is actually a worst case upper limit. Worst case means that no additional knowledge about the hit has been used, such as the observed cluster distributions in the detector that the hit belongs to, or the approximate incidence angles of the particle track producing the hit. Yet both of these things are known in practical applications, when fitting a track to a collection of hits. For example, Fig. 1(a) shows the assumed hypothetical distribution of true track position in a pixel that leads to the pitch/$\sqrt{12}$ result, compared to the actual distribution in Fig. 1(b) which shows the track positions for the case of single hit clusters in a $50 \times 50 \times 150$ μm^3 pixel sensor being crossed at normal incidence.[1] The RMS of the actual distribution shown is $0.78\times\text{pitch}/\sqrt{12}$. The reason is that tracks near the edge of the pixel will produce 2-pixel clusters instead of 1-pixel clusters. This charge sharing is related to the sensor thickness: in an infinitely thin sensor the track positions for 1-hit clusters would actually look like Fig. 1(a). The beneficial effect of knowing the cluster size distribution becomes greater for larger clusters, as will be seen later.

The goal of this paper is to survey the position resolution of binary readout pixels for a variety of pixel sizes of current and future interest, as shown in Table 1, covering the range of incidence angles found in practical applications. The incidence angle is decomposed along two directions: polar (θ) and azimuthal (ϕ) as shown in Fig. 2. Colliding beam detectors contain a central *barrel* section of cylindrical geometry with axis along the colliding beams, while fixed target as well as forward elements of colliding beam detectors use sensor planes approximately perpendicular to the particle flux. In the barrel geometry the azimuthal range is small ($\phi < 30°$) and the polar range is larger ($\theta_{max} > 45°$), while in forward planes both angles are small. Hadron colliders use the

[1] We present all results in the absence of a magnetic field. If a magnetic field is present the incidence angles relative to the sensor plane must be replaced by angles relative to the charge drift direction. The equivalent of "normal incidence" would thus be "parallel to the drift direction".

* Corresponding author at: Department of Engineering Physics, Tsinghua University, Key Laboratory of Particle and Radiation Imaging, Ministry of Education, Beijing 100084, China.
E-mail address: wangfy15@mails.tsinghua.edu.cn (F. Wang).

https://doi.org/10.1016/j.nima.2018.04.053
Received 17 November 2017; Received in revised form 25 April 2018; Accepted 25 April 2018
Available online 5 May 2018
0168-9002/

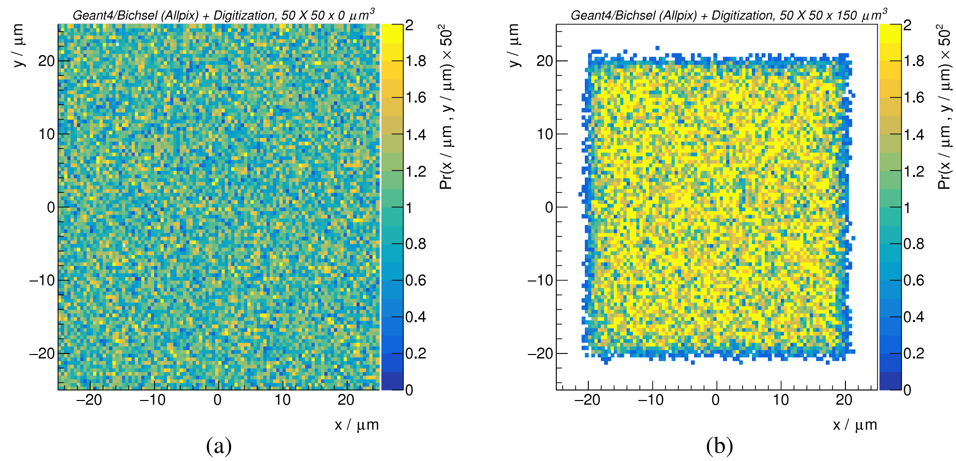

Fig. 1. Distribution of track positions in a single pixel cluster: (a) commonly assumed, which is only correct for an infinitely thin sensor; (b) actual for normal incidence tracks in a $50 \times 50 \times 150\ \mu m^3$ sensor.

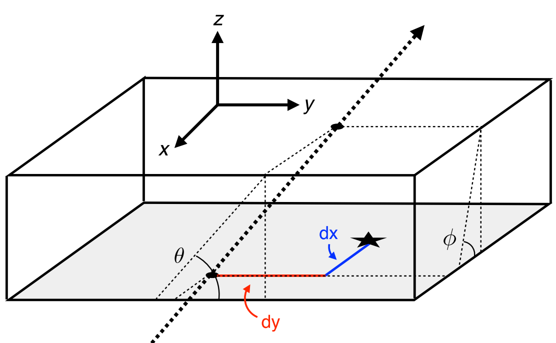

Fig. 2. Definition of coordinates and incidence angles and depiction of the residual on the sensor surface of incidence. The particle trajectory is shown as the heavy dotted line, with the sensor entrance and exit points are marked by ovals. The estimated entrance point is indicated by a star. The separation between estimated and true entrance points on the plane of the sensor surface is decomposed into dx and dy.

Table 1
Simulated pixel sensor geometries.

Pixel dimension ($x \times y$)	Sensor thickness
50 μm × 250 μm	200 μm
50 μm × 50 μm	150 μm, 100 μm
25 μm × 100 μm	150 μm, 100 μm
25 μm × 25 μm	100 μm, 50 μm
10 μm × 10 μm	20 μm
5 μm × 5 μm	10 μm
2 μm × 2 μm	10 μm, 5 μm

variable pseudorapidity $\eta \equiv -\ln(\tan(\theta/2))$ to describe the polar angle. In this study we do not simulate a particular detector geometry, but rather a single sensor in a flux of incident particles, spanning the angular ranges $0 < \phi < 50°$ and $0 < |\eta| < 2$.

We simulate rectangular as well as square pixels, as the former are often used in barrel detectors, with the long dimension of the pixel along the beam direction, which is done in order to improve position resolution in the azimuthal direction without increasing channel density. The details of our simulation are presented in Section 2. As we are exploring the limits of resolution, we do not include noise or electronic charge sharing (crosstalk) in the simulation. The impacts of noise and crosstalk, which are unavoidable in a real system, are assessed in Section 5.

2. Simulation

The simulation is based on the Geant4 package [4]. We are concerned with the intrinsic resolution for minimum ionizing charged particles and therefore simulate a monochromatic source of 20 GeV muons. For low momentum particles, the hit distance from the fitted track will be dominated by multiple scattering, and therefore this analysis is mainly of interest to relatively high momentum particles. Since the incidence angle will not be perfectly known when fitting a collection of hits, we uniformly smear the entrance angles in each simulation by 1 mrad. In terms of multiple scattering of 20 GeV muons, the RMS scattering angle when traversing 3% of a radiation length is about 0.1 mrad, which shows that the applied smearing is indeed coarse [5]. To ensure uniform illumination over at least one pixel, the source position is smeared uniformly by the pixel dimensions.

We simulate a single sensor at a time illuminated by the above source, with a variety of sensor thicknesses and pixel sizes as shown in Table 1. All simulations use a planar sensor geometry. We simulate the collection of electrons. The Bichsel model [6] is used to predict the energy loss along the particle trajectory, and we convert the energy loss to charge via $1e^- = 3.6$ eV [7]. For computational convenience we group electrons into $\mathcal{O}(10)$ clumps per pixel pitch, except for the smallest pixels simulated, for which the number of electrons per pixel pitch is already of order 10 and no clumping is needed (each electron is its own clump). Each clump is transported to the sensor surface assuming drift along the electric field plus diffusion perpendicular to the field equal to $2.5\ \mu m \times \sqrt{d/300\ \mu m}$ [7], where d is the drift length. The values chosen correspond to the diffusion length expected at −10 °C with 1 V/μm field. We assume a uniform drift field of 1 V/μm in all cases, which is above unirradiated depletion voltage for all thicknesses considered and is also consistent with saturation drift velocity [8]. Other sources of charge sharing such as electronic noise and capacitive coupling between readout chips are not considered, because the impact is checked to be small (see Section 5).

The total charge arriving at each pixel is then compared to a threshold and the pixel is considered hit if the charge is above threshold, and not hit otherwise. We use a threshold value of $1000\,e^-$ for 150 μm thick sensors and scale it linearly with sensor thickness.

3. Shape classification and RMS calculation

For each incidence angle we observe several distinct cluster shapes and for each shape we record the distribution of particle track entrance points to the sensor. The optimal position estimator of each module given the shape and incidence angle is the mean of the entrance point distribution (the estimator that minimizes the mean squared